Macromol. Symp. **2009**, 285, 81–89 DOI: 10.1002/masy.200951111

Simultaneous Deconvolution of the Molecular Weight and Chemical Composition Distribution of Polyolefins Made with Ziegler-Natta Catalysts

*Abdulaziz A. Alghyamah, João B. P. Soares**

Summary: Heterogeneous Ziegler-Natta catalysts produce polyolefins that have broad distributions of molecular weight (MWD) and chemical composition (CCD). For such broad distributions, mathematical models are useful to quantify the information provided by polyolefin analytical techniques such as high-temperature gel permeation chromatography (GPC), temperature rising elution fractionation (TREF), and crystallization analysis fractionation (CRYSTAF). In this paper, we developed a mathematical model to deconvolute the MWD and CCD of polyolefins simultaneously, using Flory's most probable distribution and the cumulative CCD component of Stockmayer's distribution. We have applied this procedure to ''model'' polyolefin resins and to one industrial linear low-density polyethylene (LLDPE) resin. The proposed methodology is able to deconvolute theoretical distributions even when random noise is added to the MWDs and CCDs, and it can be used to calculate the minimum number of active site types on heterogeneous Ziegler-Natta catalysts.

Keywords: crystallization analysis fractionation; CRYSTAF; GPC; linear low density polyethylene; gel permeation chromatography; LLDPE; temperature rising elution fractionation; TREF; Ziegler-Natta catalysts

Introduction

The molecular weight (MWD) and chemical composition (CCD) distributions of polyolefins have a significant impact on their physical and rheological properties.[1] It is, therefore, very important to develop mathematical models that quantify the information provided by polyolefin analytical techniques such as high-temperature gel permeation chromatography (GPC), crystallization analysis fractionation (CRYSTAF), and temperature rising elution fractionation (TREF). GPC is the most widely used analytical technique for MWD determination. TREF and CRYSTAF are commonly used for CCD measurement; both techniques fractionate semicrystalline polymers according to chain crystallizability in dilute solutions.[2–6] One of the main factors affecting the crystallizability of ethylene/α-olefin copolymers is their comonomer content.[3] A CCD is obtained from TREF or CRYSTAF data using a calibration curve that correlates the elution temperature of TREF (or crystallization temperature of CRYSTAF) with the comonomer molar fraction in the copolymer. As the comonomer content increases, the elution or crystallization temperature of linear low-density polyethylene (LLDPE) decreases. The calibration curve is normally linear and depends on comonomer type.[3–7]

One of the fingerprints of polyolefins made with heterogeneous Ziegler-Natta catalysts is that they have broad MWDs, and broad, and often multimodal, CCDs.[8] These broad distributions are attributed to the presence of multiple active site-types on the catalyst.[9] Mass and heat transfer resistances may also cause further broadening of these distributions under certain

---

Department of Chemical Engineering, University of Waterloo, Waterloo, Ontario, Canada N2L 3G1
E-mail: jsoares@uwaterloo.ca

Table 1.
Summary of model equations used for MWD and CCD deconvolution.

Description	Equations	
MWD of polymer made on each site type	$w_i(\log\mathrm{MW}) = 2.3026\mathrm{MW}^2\tau_\mathrm{i}^2\exp(-\mathrm{MW}\tau_\mathrm{i})$	(1)
τ_i	$\tau_i = \frac{1}{M_{ni}} = \frac{1}{r_n mw}$	(2)
MWD of the whole polymer	$W(\log\mathrm{MW}) = 2.3026\sum_{\mathrm{i}=1}^{\mathrm{n}}\mathrm{m_i}\mathrm{MW}^2\tau_\mathrm{i}^2\exp(-\mathrm{MW}\tau_\mathrm{i}^2)$	(3)
CCD of polymer made on each site type	$w_i(F) = \frac{3}{4\sqrt{2mw\beta_i\tau_i}\left[1+\frac{(F-\overline{F}_i)^2}{2mw\beta_i\tau_i}\right]^{5/2}}$	(4)
β_i	$\beta_i = \overline{F}_i(1-\overline{F}_i)\sqrt{1-4\overline{F}_i(1-\overline{F}_i)(1-r_{1i}r_{2i})}$	(5)
CCD of the whole polymer	$W(F) = \sum_{i=1}^{n} m_i \frac{3}{4\sqrt{2mw\beta_i\tau_i}\left[1+\frac{(F-\overline{F}_i)^2}{2mw\beta_i\tau_i}\right]^{5/2}}$	(6)

M_{ni}: number average molecular weight; r_n: number average chain length; F: mol fraction of comonomer; $\overline{F}_i$: average mol fraction of α-olefin comonomer; r_{1i} and r_{2i}: comonomer reactivity ratios; n: number of active site types; subscript i: site type; mw: molecular weight of the repeating unit.

polymerization conditions.[10–12] From the MWDs and CCDs of polyolefins, the minimum number of site types present on the catalyst can be predicted. The instantaneous MWD of polymer chains made on each site type can be described using Flory's most probable distribution.[13–15] Similarly, Stockmayer's bivariate distribution can be used to represent the instantaneous CCD of copolymer chains made on each site type.[16–17] Recently, Kissin et al. developed an empirical method for quantifying CRYSTAF data based on resolution of CRYSTAF curves into several elemental components, each of which representing a fraction of polymer with the same copolymer content or the same degree of stereoregularity.[18] Beigzadeh et al. studied the effect of polymerization conditions and catalyst type on the CCDs of ethylene/α-olefin copolymers made with single-site and Ziegler-Natta catalysts. They used a Monte-Carlo model to simulate the CRYSTAF profiles based on a relation between lamella thickness and crystallization temperature.[19–21] Their predicted distributions agreed well with experimental CRYSTAF profiles for the ethylene/1-octene copolymers investigated.

In this paper, we develop a novel methodology to deconvolute the MWD and CCD of polyolefins simultaneously using Flory's most probable distribution and the cumulative CCD component of Stockmayer's distribution.

Mathematical Modeling of MWD and CCD

It has been proposed that the MWD and CCD of polyolefins produced with heterogeneous Ziegler-Natta catalysts can be modeled as a weighted sum of Flory's most probable distributions and Stockmayer's distributions, respectively. Table 1 summarizes the equations that describe the MWD and CCD for each site type and for the whole polymer.[13–17]

The main objective of the proposed methodology is to deconvolute the MWD and CCD of polyolefins simultaneously, using the equations in Table 1. We have also included in our deconvolution procedure the room-temperature soluble fraction that is commonly present in LLDPE resins,[22–23] as shown in Figure 1 for a LLDPE sample with a soluble fraction of approximately 10 wt-%. We found that it is possible to achieve this goal using the analytical solution of the cumulative form of Equation (4), given below in Equation (7), in the deconvolution procedure.

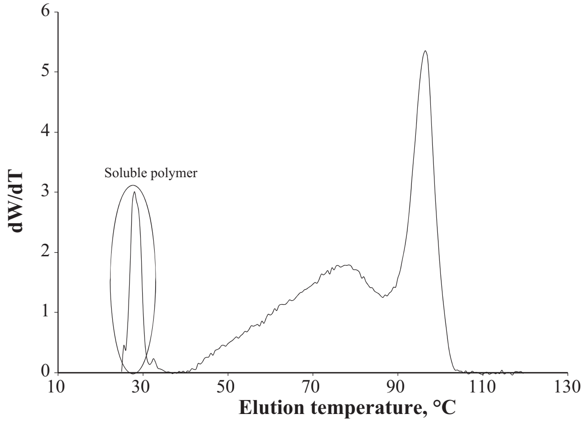

Figure 1.
CCD distribution of a LLDPE measured by TREF, showing the fraction of polymer soluble at room temperature in trichlorobenzene (TCB).

$$\begin{aligned} w_i^c(F) &= \int_{-\infty}^{F} w_i(F)dF \\ &= \frac{2\left[2mw\beta_i\tau_i+\left(F-\overline{F_i}\right)^2\right]^{5/2}+3\left(F-\overline{F_i}\right)(2mw\beta_i\tau_i)^2+5(2mw\beta_i\tau_i)\left(F-\overline{F_i}\right)^3+2\left(F-\overline{F_i}\right)^5}{4\left[2mw\beta_i\tau_i+\left(F-\overline{F_i}\right)^2\right]^{5/2}} \end{aligned} \quad (7)$$

The mass fraction of polymer produced by each site type is defined as

$$m_i = m_i^s + m_i^{ns} \quad (8)$$

where m_i is the total mass fraction of polymer made on site type i, and m_i^s and m_i^{ns} are the mass fractions of polymer that are soluble and insoluble at room temperature, respectively.

Stockmayer's bivariate distribution can be used to describe the shape of the peaks that are detected above room temperature. The soluble peak that appears in Figure 1 is not a chromatographic peak, but simply a purge peak: the area under it is proportional to the fraction of polymer that is soluble at room temperature in the solvent used during TREF fractionation. Therefore, for the soluble polymer fraction, Stockmayer's distribution can be used to predict only the mass fraction, as shown below in Equation (9),

$$m_i^s = \int_{-\infty}^{F_{crit}} w_i(F)\mathrm{d}F \quad (9)$$

where F_{crit} is the critical molar fraction of monomer below which the polymer chains are soluble at room temperature. The value of F_{crit} can be determined from the TREF calibration curve by extrapolating the curve to room temperature (35 °C in Figure 1).

The cumulative CCD for the whole resin is given by:

$$W^c(F) = \sum_{i=1}^{n} m_i^s \text{ if } F < F_{crit} \quad (10.a)$$

$$W^c(F) = \sum_{i=1}^{n} m_i^{ns} w_i^c(F) \quad \text{if } F \geq F_{crit} \quad (10.b)$$

The proposed deconvolution procedure solves Equations (3) and (10) simultaneously to determine the modeling parameters m_i, τ_i, and β_i for each site-type. The objective function, χ^2, for this non-linear optimization problem was defines as,

$$\begin{aligned} \chi^2 = \min\{&[W_{exp}(\log MW) - W_{model}(\log MW)]^2 \\ &+ [W_{exp}^c(F) - W_{model}^c(F)]^2\} \end{aligned} \quad (11)$$

where $W_{\exp}(\log MW)$ and $W_{\exp}^c(F)$are the MWD measured by GPC, and the

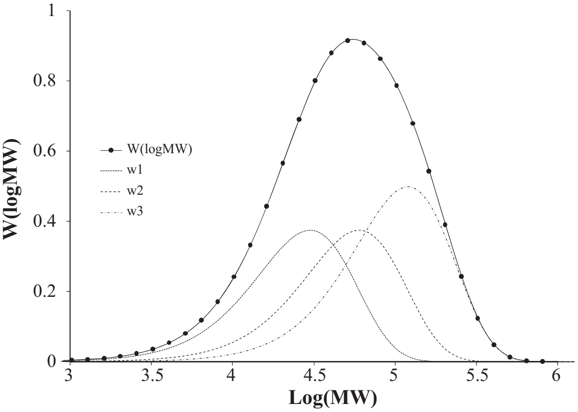

Figure 2.
MWD of a model polymer made with a 3 site-type catalyst. Model parameters: $m_1 = 0.3$, $M_{n,1} = 15\,000$; $m_2 = 0.3$, $M_{n,2} = 30\,000$; $m_3 = 0.4$, $M_{n,3} = 60\,000$.

cumulative CCD measured by TREF or CRYSTAF, respectively.

A non-linear least squares optimization routine is required to minimize the squares of the differences between the measured and predicted distributions. We have also adopted the optimization constraint that is the site types that make polymer with higher average comonomer fractions should produce polymer with lower number average molecular weights, M_n, since this is the pattern observed for all LLDPE resins made with heterogeneous Ziegler-Natta catalysts.

Results and Discussion

A ''model'' polymer has been used to test the proposed deconvolution procedure. The MWD and CCD of this polymer were simulated using a three site-type catalyst and are illustrated in Figures 2 and 3, respectively.[24]

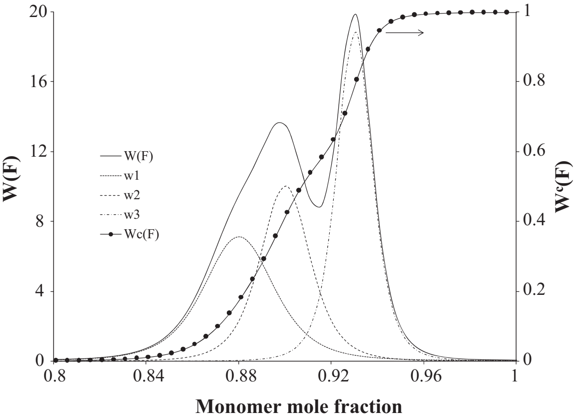

Figure 3.
CCD of a model polymer made with a 3 site-type catalyst. Model parameters: $1 - \overline{F_1} = 0.88$, $\beta_1 = 0.25$; $1 - \overline{F_2} = 0.90$, $\beta_2 = 0.25$; $1 - \overline{F_3} = 0.93$, $\beta_3 = 0.25$ ($1 - \overline{F_i}$: ethylene mole fraction).

Table 2.
Deconvolution results for the model polymer (Figures 2 and 3).

n	2 site types		3 site types			4 site types			
	1	2	1	2	3	1	2	3	4
m	0.67	0.33	0.3	0.3	0.4	0.299	10^{-4}	0.301	0.4
M_n	23,304	72,657	15,000	30,000	60,000	14,988	26,959	29,969	60,000
$1-\overline{F}$	0.894	0.930	0.88	0.9	0.93	0.879	0.888	0.899	0.929
β	0.577	0.243	0.25	0.25	0.25	0.25	0.249	0.249	0.25
χ^2	4.62		10^{-15}			0.0002			

Using these model distributions, the deconvolution procedure is started by assuming two active site types and trying to minimize the value of χ^2 defined in Equation (11). The results, as shown in Table 2, demonstrate that two site types are inadequate to represent the MWD and CCD of the model polymer. The value of χ^2 drops dramatically from 4.62 to approximately zero as the number of site types increases from 2 to 3, but remains practically the same when 4 site types are used. As expected, the best fit of the data is obtained using three site types. Table 2 shows the calculated model parameters (m_i, M_{ni}, β_i, and $1-\overline{F_i}$) using 2, 3 and 4 active site types.

Random noise was added to the MWD and CCD of the model polymer to study its effect on the model parameter values obtained by deconvolution. Figures 4 and 5 show the deconvolution results of the distributions with noise. The model describes the MWD and CCD with noise very well using three site types. The deconvolution results, shown in Table 3, demonstrate that the values of the model parameters are not significantly different than those obtained without noise.

An industrial LLDPE resin was also analyzed using the new deconvolution model. The MWD and CCD of this sample are shown in Figure 6. The TREF profile of this sample was converted into its equivalent CCD using a poly(ethylene-co-1-octene) calibration curve published in the literature.[25] The value for F_{crit} adopted in this deconvolution was 0.89.

The same deconvolution procedure discussed above was repeated for the MWD and CCD of the industrial sample, starting with 2 site types and increasing the number

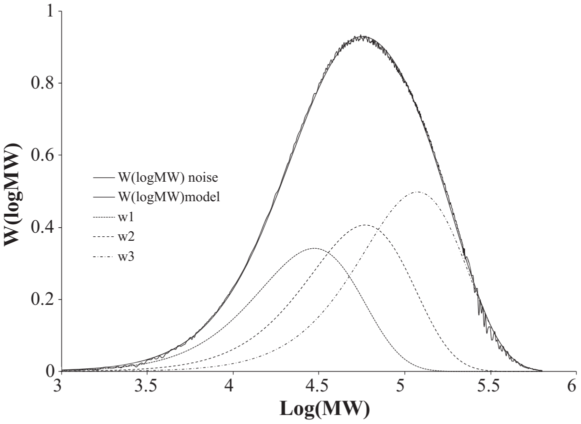

Figure 4.
Effect of random noise on MWD deconvolution using 3 site-types. $W(\log MW)noise = W(\log MW) \cdot R$, where R is a random number generated between 1 and 0.8.

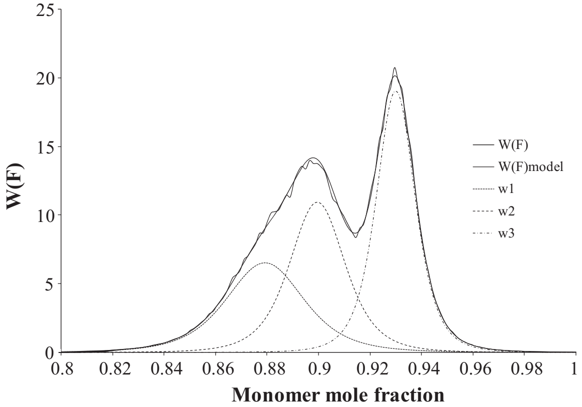

Figure 5.
Effect of random noise on CCD deconvolution results using 3 site-types. $W(F)noise = W(F) \cdot R$, where R is a random number generated between 1 and 0.8.

Table 3.
Deconvolution results with random noise.

n	1	2	3
m	0.273	0.327	0.4
M_n	14,760	29,233	59,089
$1-\overline{F}$	0.879	0.899	0.93
β	0.242	0.245	0.243

of site types until the value of χ^2 did not decrease appreciably anymore. The value of χ^2 decreased significantly as n increased from 2 to 5, as shown in Figure 7, but remained practically unchanged when 5 or 6 site-types were used, which indicates that the best representation of these distributions is obtained using 5 site types. Figures 8 and 9 show the deconvolution results for the MWD and CCD, respectively, using 5 site-types. A summary of the model parameters for this sample is given in Table 4. Since Site 1 makes polymer that is completely soluble in trichlorobenzene (TCB, the solvent used for the TREF analysis) at room temperature, it is not possible to estimate the average comonomer content and the parameter β for this site.

The instantaneous bivariate weight distribution of chain length and chemical

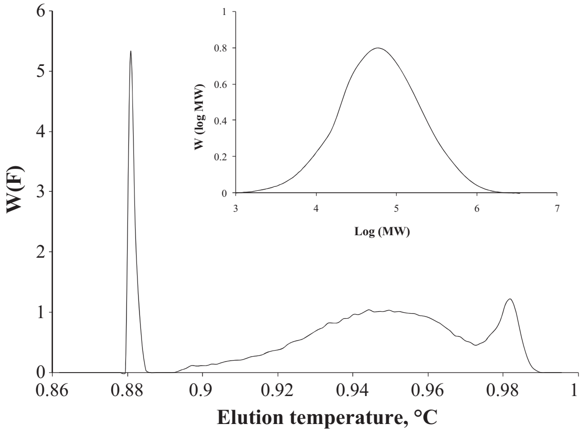

Figure 6.
CCD and MWD (insert) of a industrial LLDPE sample.

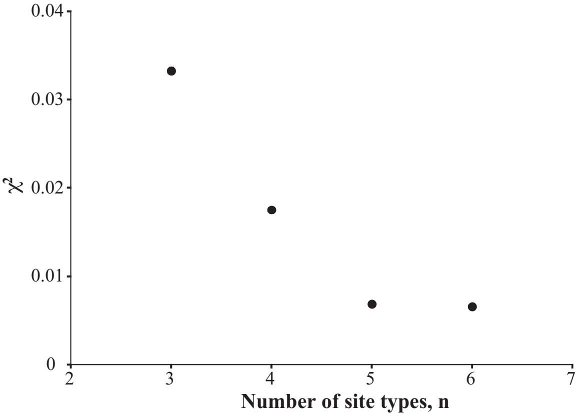

Figure 7.
Values of χ^2 for different numbers of site-types for the deconvolution of the MWD and CCD shown in Figure 6. The value of χ^2 for $n = 2$ is omitted since it is approximately 10 times larger than when $n = 3$.

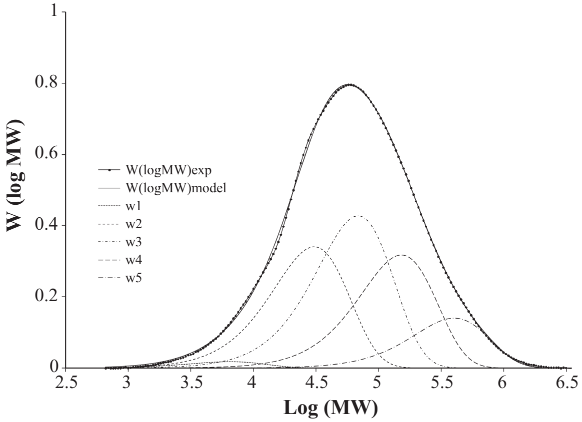

Figure 8.
MWD deconvolution results for an industrial LLDPE resin using 5 site types ($\chi^2 = 0.0045$).

composition for each site type, $w_i(r,F)$, can be described by Stockmayer's distribution (in logarithm scale)[16,24]

$$w_i(r,F) = 2.3026 \times \frac{r^2}{r_{ni}^2}\exp\left(-\frac{r}{r_{ni}}\right)\sqrt{\frac{r}{2\pi\beta_i}}\exp\left[-\frac{r(F-\overline{F}_i)^2}{2\beta_i}\right] \tag{12}$$

where r is the chain length and r_n is the number average chain length that can be obtained from M_n as shown in Equation (2). Consequently, the overall bivariate distribution can be obtained with an expression similar to Equation (10.b):

$$W(r,F) = \sum_{i=1}^{n} m_i^{ns} w_i(r,F) \quad \text{if } F \geq F_{crit} \tag{13}$$

Figure 10 shows the bivariate distribution of the LLDPE sample shown in Figure 6. Notice that the site types that produce polymer with high number average

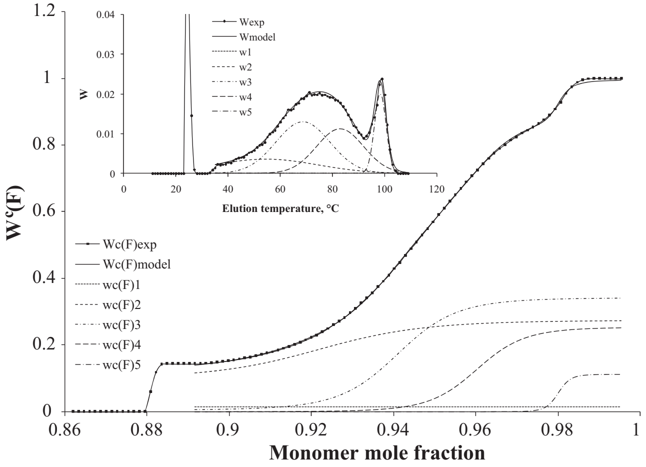

Figure 9.
Cumulative CCD and TREF curve (insert) deconvolution results for an LLDPE resin using 5 site types. Site 1 is not shown in the TREF curve since it makes polymer that is totally soluble at room temperature.

Table 4.
Deconvolution results for the LLDPE resin.

n	1	2	3	4	5
m	0.0136	0.2106	0.3412	0.3050	0.1296
m^{ns}	0	0.1258	0.3395	0.3049	0.1296
m^{s}	0.0136	0.0848	0.0016	0.0001	0
M_n	3,570	17,404	38,422	84,408	213,813
$1-\overline{F}$		0.9272	0.9530	0.9650	0.9804
β		0.5209	0.3544	0.3541	0.0678

chain length make polymer with the lower comonomer content, as shown dramatically in Figure 10.

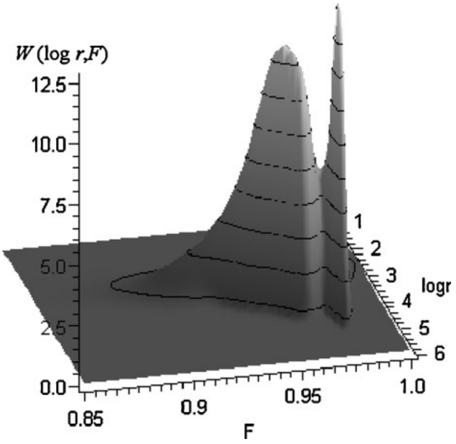

Figure 10.
Predicted bivariate distribution of chain length and chemical composition distributions of an industrial LLDPE sample.

Conclusions

We developed a new procedure to simultaneously deconvolute the MWD and cumulative CCD of polyolefins made with heterogeneous Ziegler-Natta catalysts, including the room temperature soluble fraction. The model can be used to predict the minimum number of site types required to describe the MWD and CCD of a polyolefin sample for mathematical modeling applications. We applied this novel technique to an industrial LLDPE resin and showed that it can be used to estimate the number average molecular weight, average comonomer mole fraction, and mass fraction of soluble and non-soluble polymer chains made on each site.

Acknowledgements: The authors would like to thank Dow Chemical for kindly providing them with CRYSTAF, TREF, and GPC analyses of the sample reported in this article.

[1] M. Gronder, *J. Plast. Film Sheeting* **2001**, *17*, 53.
[2] J. B. P. Soares, A. E. Hamielec, *Macromol. Theory Simul.* **1995**, *4*, 305.
[3] S. Anantawaraskul, J. B. P. Soares, P. M. Wood-Adams, *Adv. Polym. Sci.* **2005**, *182*, 1.
[4] J. B. P. Soares, A. E. Hamielec, *Polymer* **1995**, *36*, 1639.
[5] B. Monrabal, *J. Polym. Sci.* **1994**, *52*, 491.
[6] J. B. P. Soares, B. Monrabal, J. Nieto, J. Blanco, *J. Macromol. Chem. Phys.* **1998**, *199*, 1917.
[7] E. P. Savitski, G. B. Caflisch, C. M. Killian, M. Meadows, J. H. Merkley, B. J. Huff, *J. Appl. Polym. Sci.* **2003**, *90*, 722.
[8] V. V. Vickroy, H. Scheider, R. F. Abbott, *J. Appl. Polym. Sci.* **1993**, *50*, 551.
[9] J. C. Chien, C. Kuo, T. Ang, *J. Polym. Sci., Part A: Polym. Chem.* **1985**, *23*, 723.
[10] U. Zucchini, G. Cecchin, *Adv. Polym. Sci.* **1983**, *51*, 101.
[11] S. Floyd, R. Heiskanen, W. H. Ray, *Chem. Eng. Prog.* **1988**, *84*, 56.
[12] J. B. P. Soares, A. E. Hamielec, *Polym. React. Eng.* **1995**, *3*, 261.
[13] Y. V. Kissin, *Makromol. Chem., Macromol. Symp.* **1993**, *66*, 83.
[14] Y. V. Kissin, *J. Polym. Sci., Part A: Polym. Chem.* **1995**, *33*, 227.
[15] J. B. P. Soares, A. E. Hamielec, *Polymer* **1995**, *36*, 2257.
[16] W. H. Stockmayer, *J. Chem. Phys.* **1945**, *13*, 199.
[17] J. B. P. Soares, R. F. Abbott, J. N. Willis, X. Liu, *Macromol. Chem. Phys.* **1996**, *197*, 3383.
[18] Y. V. Kissin, H. A. Fruitwala, *J. Appl. Polym. Sci.* **2007**, *106*, 3872.
[19] D. Beigzadeh, J. B. P. Soares, T. A. Duever, *J. Appl. Polym. Sci.* **2001**, *80*, 2200.
[20] J. B. P. Soares, D. Beigzadeh, T. A. Duever, A. A. da Silva Filho, *Polym React Eng.* **2000**, *8*, 241.
[21] D. Beigzadeh, PhD thesis, University of Waterloo, Canada, **2000**.
[22] Y. L. Yu, C. C. Tso, P. J. DesLauriers, *J. Appl. Polym. Sci.* **2006**, *100*, 4992.
[23] C. C. Tso, P. J. DesLauriers, *Polymer* **2004**, *45*, 2657.
[24] J. B. P. Soares, L. C. Simon, In T. Meyer, J. Keurentjes Eds, *Handbook of Polymer Reaction Engineering*, Wiley-VCH, Weinheim, **2005**, pp. 365–430.
[25] A. A. da Silva Filho, J. B. P. Soares, G. B. de Galland, *Macromol. Chem. Phys.* **2000**, *201*, 1226.